Received 9 January 2020; revised 19 February 2020; accepted 4 March 2020. Date of publication 11 March 2020; date of current version 19 March 2020. The review of this article was arranged by Editor S. Ikeda.

Digital Object Identifier 10.1109/JEDS.2020.2979293

Current Pulses to Control the Conductance in RRAM Devices

HÉCTOR GARCÍA, SALVADOR DUEÑAS, ÓSCAR G. OSSORIO, AND HELENA CASTÁN

Department of Electronics, University of Valladolid, 47011 Valladolid, Spain

CORRESPONDING AUTHOR: H. GARCÍA (e-mail: hecgar@ele.uva.es)

This work was supported by the Spanish Ministry of Economy and Competitiveness and the FEDER Program through project under Grant TEC2017-84321-C4-2-R.

ABSTRACT Due to the high number of reachable conductance levels in resistive switching devices, they are good candidates to implement artificial synaptic devices. In this work, we have studied the control of the intermediate conductance levels in HfO_2-based MIM capacitors using current pulses. The set transition can be controlled in a linear way using this kind of signal. The potentiation characteristic is not affected by the pulse length due to the filament formation takes place in very short times. This behavior does not allow using identical pulses to obtain the potentiation characteristic. The transient response of the devices when applying current pulses showed the filament formation is characterized by a peak in the voltage transient signal. No depression characteristic can be obtained using current signals due to the abrupt reset transition. However, the depression characteristic can be obtained using voltage pulses, so combining both signals should allow control the synaptic weight in an appropriate way.

INDEX TERMS Conductive filament, multilevel storage, resistive switching memory (RRAM), synaptic devices.

I. INTRODUCTION

The resistive switching (RS) phenomenon, first reported in 1962 [1], has got a wide interest due to its application to store information in resistive random-access memories (RRAMs) [2], [3]. These devices consist of an insulating layer interposed between two metal electrodes, and exhibit memory when operating as a two terminal variable resistor, due to a conductive filament (CF) between both electrodes, which can be formed (set operation) obtaining a low resistance state (LRS), and dissolved (reset operation) obtaining a high resistance state (HRS). As the thickness of the conductive filament can be controlled in different ways, these devices actually show continuously variable conductance values [4].

Neuromorphic systems are inspired in the way the human brain processes the information [5], [6]. In these systems, synapses are responsible for the connection of the enormous number of neurons. The synaptic weight between two neurons is adjusted by the ionic flow through them, and the adaptation of synaptic weights enables the biological systems to learn and function properly [7]. Similar to biological synapses, the conductance value of a RRAM device can be adjusted by controlling the charge flowing through it. Due to their fast speed, low power consumption and scalability, RRAM devices are a promising approach for artificial synapses [8].

In a previous work, we studied the control of the conductance states in HfO_2-based metal-insulator-metal (MIM) capacitors applying voltage pulses [9]. We obtained linear depression characteristics, but a non-linear potentiation characteristic due to the abrupt set transition. However, linear potentiation characteristics have been observed in HfO_2-based capacitors when varying the current compliance in voltage ramps [10]. In this work, we studied the control of intermediate conductance states in similar devices using current pulses instead of the conventional voltage pulses. Using this kind of signal, a linear potentiation characteristic is achieved, although no depression characteristic can be obtained using current pulses. We have also studied transient characteristics of the set transition: the closure and broadening of the CF is characterized by a maximum in the transient signal, and is fast enough

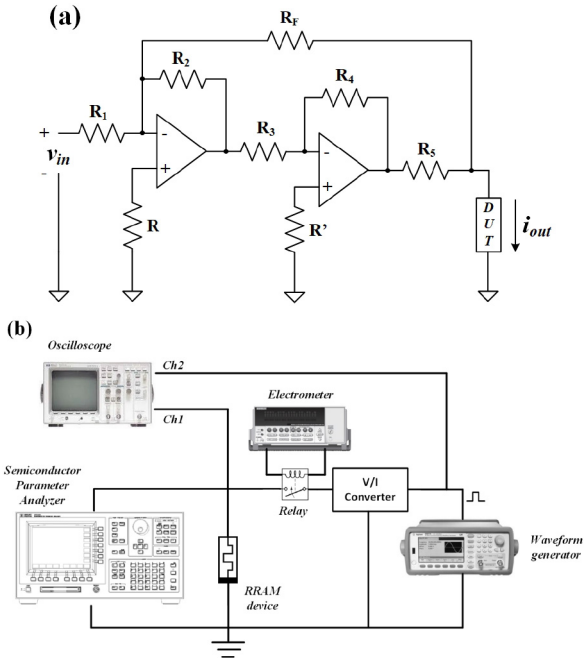

FIGURE 1. **Electrical circuit corresponding to the home-made voltage to current converter (a) and experimental setup (b).**

not to observe accumulative behavior in the limits of our experiment.

II. EXPERIMENTAL

A. DEVICE FABRICATION

TiN/Ti/10-nm HfO_2/W capacitors were used in this work. Atomic layer deposition (ALD) technique was used to grow the insulator at 225 °C. The precursors used were TDMAH and water for hafnium and oxygen respectively. Nitrogen was used both as carrier and purge gas. The top electrode consists of a 200 nm TiN layer and a 10 nm Ti layer, and the bottom electrode consists of a 200 nm W layer. Electrodes were deposited by magnetron sputtering. The resulting structures used are square cells of 40×40 μm^2.

B. EXPERIMENTAL SETUP

An HP 4155B Semiconductor Parameter Analyzer performed the non-transient voltage and current measurements. An Agilent 33500B Series waveform generator applied voltage pulses, that can be converted to current pulses using a home-made voltage to current converter. The electrical circuit corresponding to our V/I converter has been represented in Fig. 1a. Using a relay in series with the V/I converter, the device under test (DUT) can be disconneted from the converter so the HP 4155 Semiconductor Parameter Analyzer can perform the conductance measurements. An HP54615B digital oscilloscope was used to record the transient signals in transient measurements. In order to record current transients after applying voltage pulses, we used a home-made I/V converter, and the transients where observed in the HP54615B oscilloscope. The complete experimental setup is shown in Fig. 1b. The oscilloscope is not conneted for the non-transient measurements. All the measurements where computer controlled, and have been carried out at room temperature.

III. RESULTS AND DISCUSSION

The forming process was carried out using a current sweep instead of a voltage sweep, as shown in Fig. 2a. When the conductive filament is formed, the voltage that drops across the device suddenly decreases applying the same current, so the power dissipated by the sample decreases. Using this kind of signal, it is no necessary the use of a compliance in the forming process. After the forming was performed, we measured 50 voltage-current (V-I) loops, shown in Fig. 2b, obtaining bipolar RS. Using a voltage compliance in the reset transition is mandatory; otherwise, irreversible oxide breakdown takes place due to a sudden increase in the power dissipated by the structure. We then recorded V-I curves increasing the maximum positive current values applied from one loop to the next one. Fig. 2c shows the conductance values obtained for each loop, clearly showing the existence of intermediate conductance states. The device becomes more conductive for higher currents. This trend, already observed in HfO_2-based capacitors [11], is due to an increase in the thickness of the CF, as verified using computer simulations [12]. Increasing the maximum negative current values does not allow us to obtain intermediate conductance states due to the abrupt disruption of the CF when applying current instead of voltage to our device.

Since controlling the thickness of the CF using current ramps has been proved, we applied current pulses (a more suitable signal as neuromorphic systems work as spike-based circuits [13]) to obtain the potentiation characteristic. The pulses length was 50 μs, and the amplitude was linearly increased from 0 mA to 5.8 mA. The sample was carried out to the HRS and then 200 pulses were applied. After each pulse, the conductance value was measured, as represented in Fig. 3a. A minimum current amplitude is required to form the filament, and after this value is reached, a clearly linear potentiation characteristic is observed. We obtained better potentiation characteristics using current pulses than voltage pulses. Some solutions have been proposed when using voltage pulses: employing two RRAM devices with opposite weight contribution [14] or applying a proper reset pulse after the potentiation one [15]; the first attempt requires more complex devices, and the second one more complex peripheral circuitry. As we can also observe, the conductance values obtained in our samples are higher than the values used in typical RRAM applications. We have not tried to obtain lower current values, for example, reducing the current in the forming process, due to problems in the transient measurements that are presented later: as we can observe in Fig. 1b, for very high RRAM resistance values the current flowing through the V/I converter can be divided due to the oscilloscope channel 1 impedance, so no accurate transient measurements could be obtained.

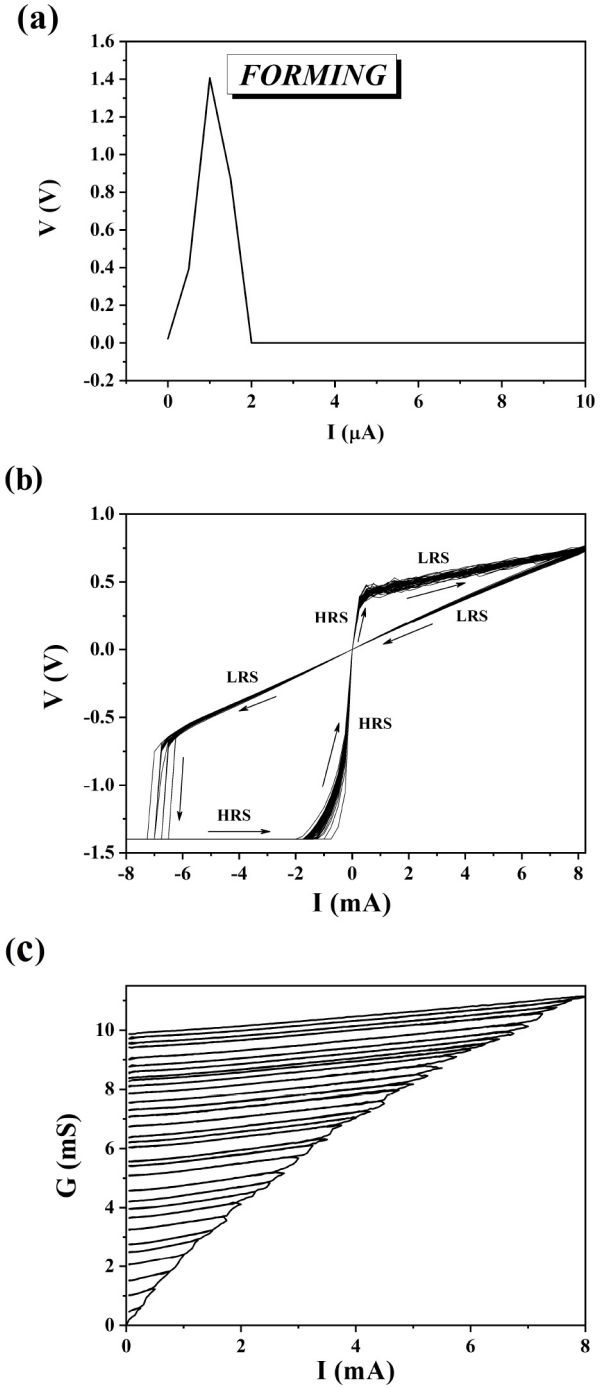

FIGURE 2. Forming process (a), V-I resistive switching loops showing HRS and LRS states (b) and G-I characteristics when increasing the maximum current (c).

Anyway, measurements carried out in a very similar samples demonstrated the RRAM devices can be programed varying the current compliance, and using lower operating currents [10]. So the method proposed here should be able to be used for lower operating currents, at least for samples showing the same CF formation mechanism, oxygen vacancy clusters [16].

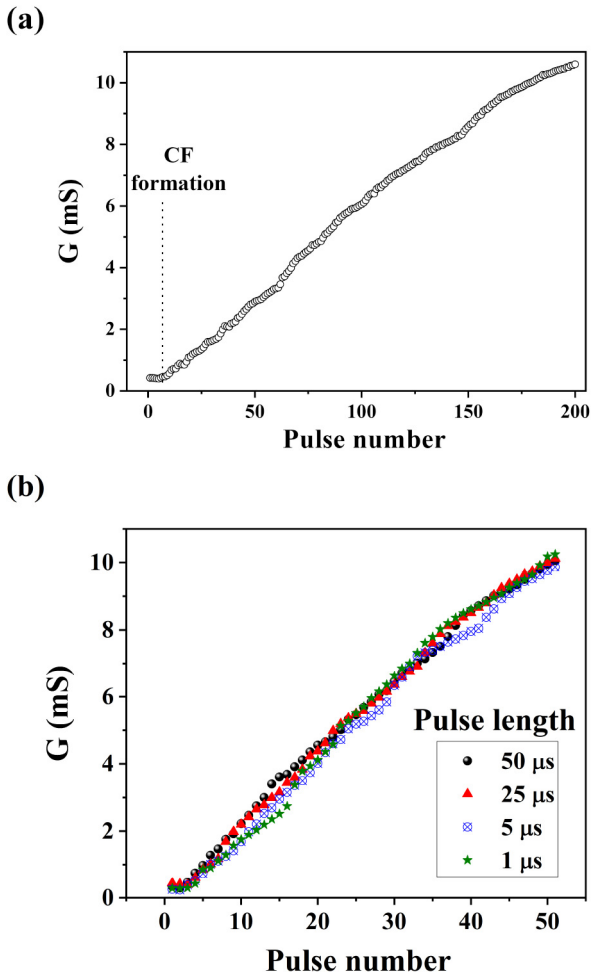

FIGURE 3. Potentiation characteristic applying current pulses, using the same (a) and different pulse lengths (b).

When using voltage pulses, simulations demonstrated the final conductance value has a strong relationship with the pulse length [17]. We observed a higher number of pulses was required to reach the same final synaptic weight when applying voltage pulses, giving place to an accumulative process, although the potentiation characteristic obtained was not linear [9]. In order to check this behavior for current pulses, we applied three series of 50 pulses with different pulse lengths, from 1 μs to 50 μs, increasing the amplitude from 0 mA to 5.8 mA. Results are represented in Fig. 3b, and no significant differences are observed for the different series. It looks like the CF formation and widening is faster than the narrowest pulse. This has been confirmed by applying pulses keeping the current amplitude constant, and is shown in Fig. 4: four series of identical pulses were applied to the capacitors, where the pulse amplitude is different for each serie. The pulse length is 5 μs for all pulses. Unlike the voltage pulses, current pulses do not show an accumulative behavior; the first pulse increases the conductance to the final expected value. This difference can be explained because in the case of voltage pulses, the resistance

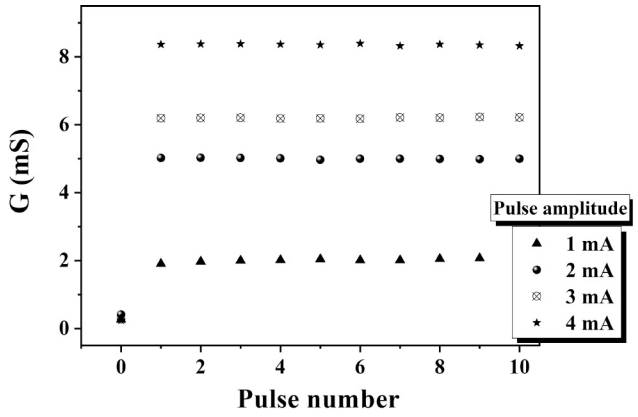

FIGURE 4. **Potentiation characteristic applying identical current pulses for each series. The pulse amplitude is different for each series.**

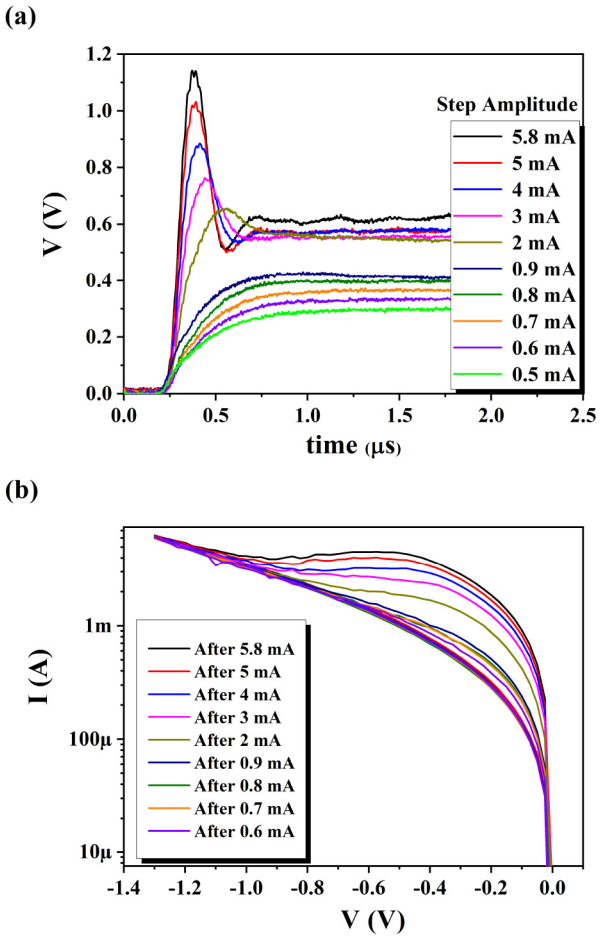

FIGURE 5. **Transient response when applying current steps with different amplitudes (a) and I-V characteristics after the current steps (b).**

value of our device decreases (potentiation characteristic) or increases (depression characteristic) as the pulses are applied, so keeping the voltage constant, the current flowing through the device increases (potentiation characteristic) or decreases (depression characteristic) for consecutive pulses.

We studied the transient response recording voltage transients when applying current steps to our devices. Fig. 5a shows the transient response when current steps with different amplitudes were applied, with devices initially in the HRS. The CF closure is characterized by a peak in the voltage signal: after reaching a high enough voltage value, the CF is suddenly closed, decreasing the resistance value, and hence, decreasing the voltage that drops across the device. The maximum voltage values reached in the peak are higher than the corresponding values obtained from V-I curves shown in Fig. 2b. The latter case does not correspond to a transient measurement, and hence, the filament is closed at lower current values and it only gets thicker as the current increases. For low amplitude pulses, no peak in the voltage signal is observed, what means the CF is not closed (the gap between the electrode and the tip of the filament remains). This is verified in Fig. 5b, which shows I-V curves measured after each current step. For low pulse amplitudes, the device clearly remains in the HRS, although the conductivity value can be slightly increased due to a reduction in the gap between the tip of the CF and the electrode [12]. It is worth mentioning that the increase in the rise time of the transient observed in Fig. 5a as the pulse amplitude decreases is only a measurement artifact due to the increased final resistance at the output of the V/I converter.

We studied the transient response when decreasing the pulse length. For this purpose, we applied current pulses with 5 mA amplitude and decreasing lengths. Fig. 6a and Fig. 6b show the voltage response to a pulse of 1 μs and 500 ns length respectively. Black line corresponds to the voltage transient, and blue line corresponds to the signal applied to the input of the V/I converter. There exists a voltage peak, characteristic of the filament formation. The minimum in the transient signal after the peak is due to the measurement system, so not related to the behavior of the device. Fig. 6c shows the response to a 200 ns length pulse, and no similar peak in the voltage signal is observed. After each pulse, an I-V measurement was carried out to know the final state (see Fig. 6d). Although no peak was observed for the 200 ns pulse, the final state is the same for the three pulses. As shown in Fig. 6c, the rise time of the current signal applied to the device, which is due to the V/I converter, is not negligible for short pulse lengths. The transient voltage signal reaches the maximum value (the same value that in Fig. 6a and Fig. 6b) just when the negative edge of the pulse takes place. We are not able to apply shorter pulses due to the limitation of our converter: the rise time would be larger than the pulse length. Thus, applying current pulses, the CF is formed in less time that our experimental set-up can measure. This feature allows the use of very short current pulses with an artificial synapse when potentiation the synaptic weight, obtaining fast switching speeds.

The mechanisms involved in the filament evolution depends on the process taking place, set or reset, as proved by different physical models [18], [19]. For comparison, we have represented the transient response to depression

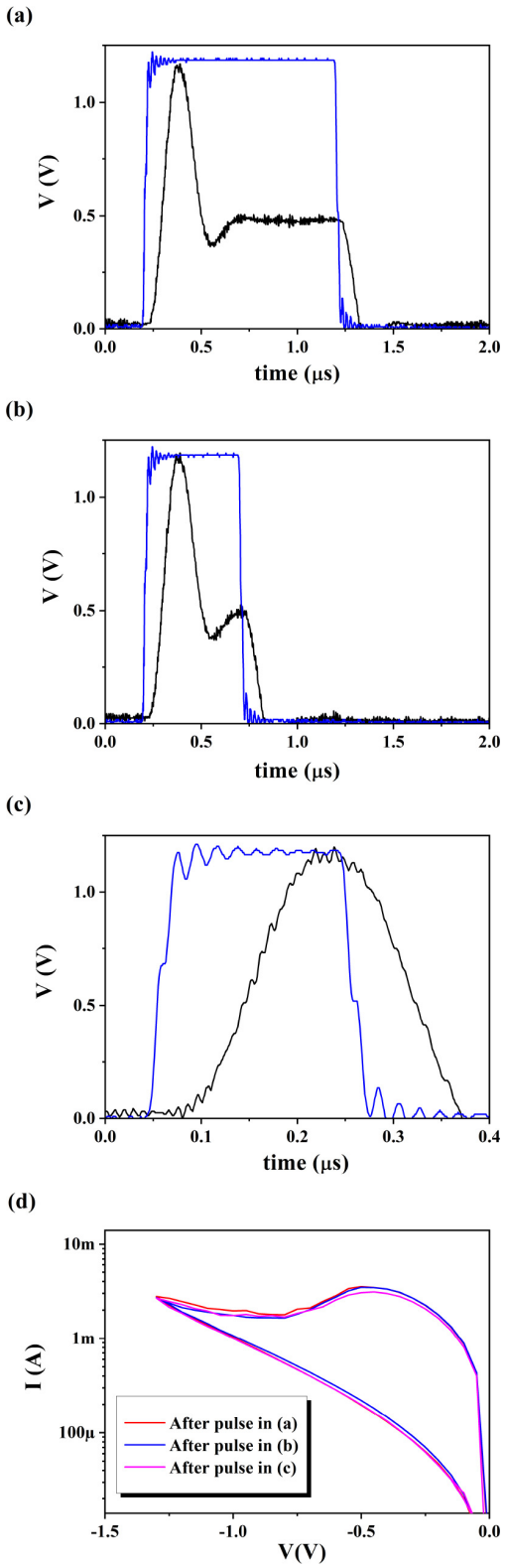

FIGURE 6. Transient response after applying a current pulse of 1 μs length (a), 500 ns length (b), and 200 ns length (c), and I-V characteristics after applying the current pulses (d).

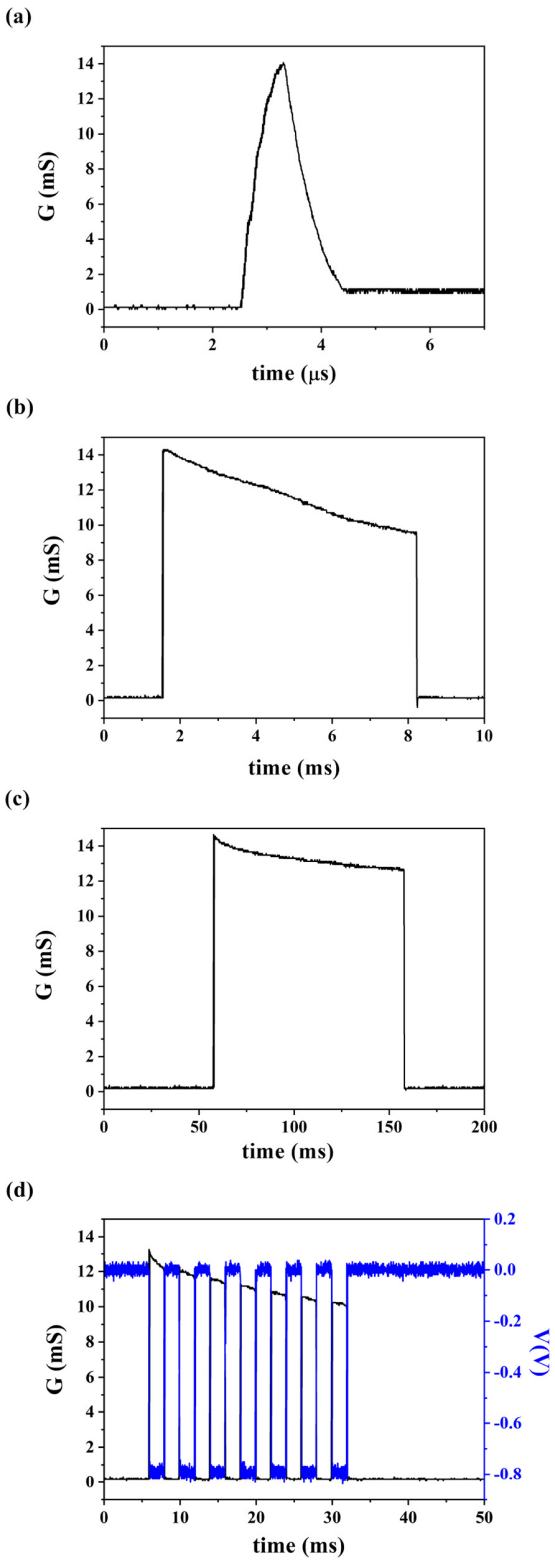

FIGURE 7. Transient response after applying a depression voltage pulse with amplitude of −1.2 V amplitude (a), −0.8 V (b), and −0.7 V (c), and accumulative process when applying voltage pulses (d).

voltage signals. Fig. 7a, Fig. 7b and Fig. 7c show the conductance response to a depression voltage step with amplitude of −1.2 V, −0.8 V and −0.7 V respectively. Conductance decreases when the CF is disrupted. We observe a voltage-time dilemma phenomenon (higher voltage amplitudes corresponds to short switching times and vice-versa),

already observed and modeled [18]. However, this slow transition allows obtaining an accumulative behavior when applying identical voltage pusles, as shown in Fig. 7d, where seven identical depression voltage pulses are applied to the device, and the conductance value decreases continuously for the consecutive pulses.

IV. CONCLUSION

The use of current pulses instead of the conventional voltage pulses enables controlling the thickness of the conductive filament in HfO_2-based RRAM devices when the set transition takes place, and hence, the control of the conductivity state of these devices. However, controlling the conductive filament removal in the reset transition is not possible using this kind of signals due to the abrupt reset transition. A peak in the voltage response when applying current pulses allows us to detect the closure of the conductive filament in the set transition. The filament formation takes place in very short times, what inhibits an accumulative behavior of the pulses: only one pulse is enough to reach the final conductance state. Therefore, it is not possible to apply identical current pulses to control the thickening of the filament as using voltage pulses in the reset transition to dissolve the filament. In summary, when using RRAM devices as artificial synapses, the use of current pulses is a possible approach to obtain linear potentiation characteristics, although the use of this kind of signal does not allow us obtaining the depression characteristic. However, as linear depression characteristics have been observed applying voltage, we could control the synaptic weight in a better way using both kind of electrical signals. Of course, this way of operation still has drawbacks, not analyzed in this work: the peripheral circuitry required to generate both current and voltage pulses would be probably more complex, which may involve larger chip sizes and delays when changing from voltage to current pulses and vice versa.

ACKNOWLEDGMENT

The authors would like to acknowledge Prof. Campabadal group from the Institute of Microelectronics of Barcelona (IMB-CSIC, Spain) for providing the samples of this study.

REFERENCES

[1] T. E. Hickmott, "Low-frequency negative resistance in thin anodic oxide films," *J. Appl. Phys.*, vol. 33, no. 9, pp. 2669–2682, Sep. 1962, doi: 10.1063/1.1702530.

[2] D. Ielmini, "Resistive switching memories based on metal oxides: Mechanisms, reliability and scaling," *Semicond. Sci. Technol.*, vol. 31, no. 6, Jun. 2016, Art. no. 063002, doi: 10.1088/0268-1242/31/6/063002.

[3] T.-C. Chang, K.-C. Chang, T.-M. Tsai, T.-J. Chu, and S. M. Sze, "Resistance random access memory," *Mater. Today*, vol. 19, no. 5, pp. 254–264, Jun. 2016, doi: 10.1016/j.mattod.2015.11.009.

[4] H. Castán *et al.*, "Analysis and control of the intermediate memory states of RRAM devices by means of admittance parameters," *J. Appl. Phys.*, vol. 124, no. 15, Oct. 2018, Art. no. 152101, doi: 10.1063/1.5024836.

[5] C. Sung, H. Hwang, and I. K. Yoo, "Perspective: A review on memristive hardware for neuromorphic computation," *J. Appl. Phys.*, vol. 124, no. 15, Oct. 2018, Art. no. 151903, doi: 10.1063/1.5037835.

[6] B. Rajendran and F. Alibart, "Neuromorphic computing based on emerging memory technologies," *IEEE J. Emerg. Sel. Topics Circuits Syst.*, vol. 6, no. 2, pp. 198–211, Jun. 2016, doi: 10.1109/JETCAS.2016.2533298.

[7] S. Song, K. D. Miller, and L. F. Abbott, "Competitive Hebbian learning through spike-timing-dependent synaptic plasticity," *Nat. Neurosci.*, vol. 3, no. 9, pp. 919–926, Sep. 2000, doi: 10.1038/78829.

[8] J. Woo, D. Lee, Y. Koo, and H. Wang, "Dual functionality of threshold and multilevel resistive switching characteristics in nanoscale HfO_2-based RRAM devices for artificial neuron and synapse elements," *Microelectron. Eng.*, vol. 182, pp. 42–45, Oct. 2017, doi: 10.1016/j.mee.2017.09.001.

[9] H. García, O. G. Ossorio, S. Dueñas, and H. Castán, "Controlling the intermediate conductance states in RRAM devices for synaptic applications," *Microelectron. Eng.*, vol. 215, Jul. 2019, Art. no. 110984, doi: 10.1016/j.mee.2019.110984.

[10] M. Pedro *et al.*, "Tuning the conductivity of resistive switching devices for electronic synapses," *Microelectron. Eng.*, vol. 178, pp. 89–92, Jun. 2017, doi: 10.1016/j.mee.2017.04.040.

[11] F. Nardi, S. Larentis, S. Balatti, D. C. Gilmer, and D. Ielmini, "Resistive switching by voltage-driven ion migration in bipolar RRAM—Part I: Experimental study," *IEEE Trans. Electron Devices*, vol. 59, no. 9, pp. 2461–2467, Sep. 2012, doi: 10.1109/TED.2012.2202319.

[12] G. González-Cordero *et al.*, "Analysis of resistive switching processes in TiN/Ti/HfO_2/W devices to mimic electronic synapses in neuromorphic circuits," *Solid-State Electron.*, vol. 157, pp. 25–33, Jun. 2019, doi: 10.1016/j.sse.2019.04.001.

[13] S. H. Jo, T. Chang, I. Ebong, B. B. Bhadviya, P. Mazumder, and W. D. Lu, "Nanoscale memristor device as synapse in neuromorphic systems," *Nano Lett.*, vol. 10, no. 4, pp. 1297–1301, Apr. 2010, doi: 10.1021/nl904092h.

[14] G. W. Burr *et al.*, "Experimental demonstration and tolerancing of a large-scale neural network (165 000 synapses), using phase-change memory as the synaptic weight element," in *Proc. IEEE Int. Electron Devices Meeting (IEDM)*, San Francisco, CA, USA, 2014, pp. 1–4, doi: 10.1109/IEDM.2014.7047135.

[15] K. Moon *et al.*, "RRAM-based synapse devices for neuromorphic systems," *Faraday Discuss.*, vol. 213, pp. 421–451, Feb. 2019, doi: 10.1039/C8FD00127H.

[16] G. González-Cordero *et al.*, "A physically based model for resistive memories including a detailed temperature and variability description," *Microelectron. Eng.*, vol. 178, pp. 26–29, Jun. 2017, doi: 10.1016/j.mee.2017.04.019.

[17] Y. Li *et al.*, "Investigation on the conductive filament growth dynamics in resistive switching memory via a universal Monte Carlo simulator," *Sci. Rep.*, vol. 7, Sep. 2017, Art. no. 11204, doi: 10.1038/s41598-017-11165-5.

[18] P. Huang *et al.*, "A physics-based compact model of metal-oxide-based RRAM DC and AC operations," *IEEE Trans. Electron Devices*, vol. 60, no. 12, pp. 4090–4097, Dec. 2013, doi: 10.1109/TED.2013.2287755.

[19] X. Guan, S. Yu, and H.-S. P. Wong, "A SPICE compact model of metal oxide resistive switching memory with variations," *IEEE Electron Device Lett.*, vol. 33, no. 10, pp. 1405–1407, Oct. 2012, doi: 10.1109/LED.2012.2210856.